ACS OMEGA

http://pubs.acs.org/journal/acsodf

Article

Dual-Surfactant-Capped Ag Nanoparticles as a Highly Selective and Sensitive Colorimetric Sensor for Citrate Detection

Samy M. Shaban, Jun Young Lee,* and Dong-Hwan Kim*

Cite This: *ACS Omega* 2020, 5, 10696−10703

Read Online

ACCESS | Metrics & More | Article Recommendations | Supporting Information

ABSTRACT: A colorimetric sensor for the detection of citrate ions is reported here using dual-surfactant-capped Ag nanoparticles (dual-AgNP sensor). A mixture of cetyl trimethyl ammonium bromide and a newly prepared gemini nonionic (GFEO) surfactant was used as a capping agent to synthesize dual-surfactant-capped Ag NPs for selective and sensitive citrate detection. The GFEO surfactant was designed with a specific chemical structure to provide strong binding with citrate for selective and sensitive detection. The developed dual-AgNP sensor showed extremely high selectivity toward citrate even in the presence of interfering species. Quantitative detection of citrate was carried out based on the changes in UV−vis absorbance and naked-eye readout. After optimization, the dual-AgNP sensor exhibited a visual detection limit of 25 μM and a low limit of detection of 4.05 nM with a UV−vis spectrometer. The developed citrate sensor performed well with a urine sample, with a high recovery of 99.6%. The prepared solution sensor was constructed on a paper-based analytical device.

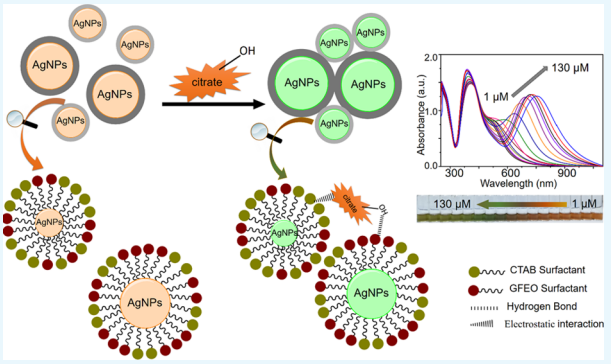

1. INTRODUCTION

Although little attention has been paid to the quantity of citrate ingested from common products including foods, cosmetics, and pharmaceuticals,[1−3] the citrate concentration is important in the human body. For instance, the citrate concentration in urine is related to kidney dysfunctions such as nephrocalcinosis and nephrolithiasis,[4,5] and a decrease in the citrate concentration in the prostatic fluid from the normal level of 50−200 to 2−20 mM is considered to be a clinical indicator of prostate cancer.[6,7] Therefore, monitoring of the citrate concentration is necessary not only for clinical diagnosis, but also for general monitoring of health.[8]

Several methods have been developed for citrate anion detection, including ion-exchange chromatography, high-performance liquid chromatography with UV detection (HPLC−UV), gas chromatography, fluorimetry, magnetic resonance spectroscopy, potentiometry, cyclic voltammetry, and electrochemical sensing.[9−11] Lately, to develop simple and convenient citrate sensors, hydrogen bonding and electrostatic interactions between an organic receptor and citrate have been studied.[3,12] However, these organic receptor-based sensors can only be applied to a nonaqueous phase assay because of the detrimental hydrogen bonding between organic receptors and water in aqueous phases.[13] In this regard, a chemosensor based on the indicator assay was developed to avoid interactions between organic receptors and water[14−16] and it was intrinsically sensitive to metal cations. As a follow-up study, the metal cations and receptor were replaced with metallic nanoparticles (NPs) and a surfactant, respectively, to avoid interactions between the metal cations and water.[17] Nonetheless, a sensitive and stable citrate detection platform is needed for the detection of minute concentrations of citrate in biological samples.

Surfactants have been widely used in the preparation of NPs because they are electron-rich and provide good chelating centers for improving the stability of NPs synthesized in a solution.[18] One of the common surfactants for the synthesis of metallic NPs is a gemini surfactant, which consists of two hydrophobic tails and two hydrophilic heads connected by a spacer.[19,20] Gemini surfactants are characterized by their relatively low critical micelle concentrations and high efficiency in decreasing the surface and interfacial tensions of water compared to conventional monomeric surfactants.[21] These properties provide a high adsorption affinity toward the surface of metal NPs for high stabilization.[22,23]

In this work, we developed a colorimetric detection platform for citrate using AgNPs. The AgNPs are capped with two surfactants: cetyl trimethyl ammonium bromide (CTAB) having positive quaternary nitrogen and a newly synthesized gemini (GFEO) surfactant containing multiple carbonyls and

Received: December 9, 2019
Accepted: March 23, 2020
Published: May 7, 2020

https://dx.doi.org/10.1021/acsomega.9b04199
ACS Omega 2020, 5, 10696−10703

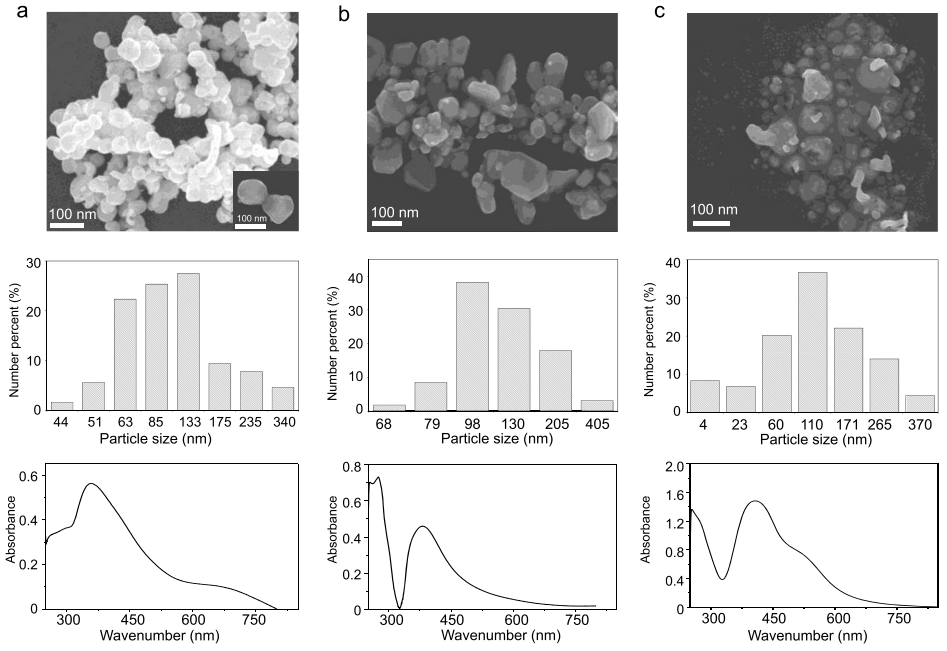

Figure 1. SEM image (top), particle size distribution (middle), and UV−vis spectrum (bottom) of the as-prepared (a) CTAB-AgNPs, (b) GFEO-AgNPs, and (c) dual-AgNP sensor.

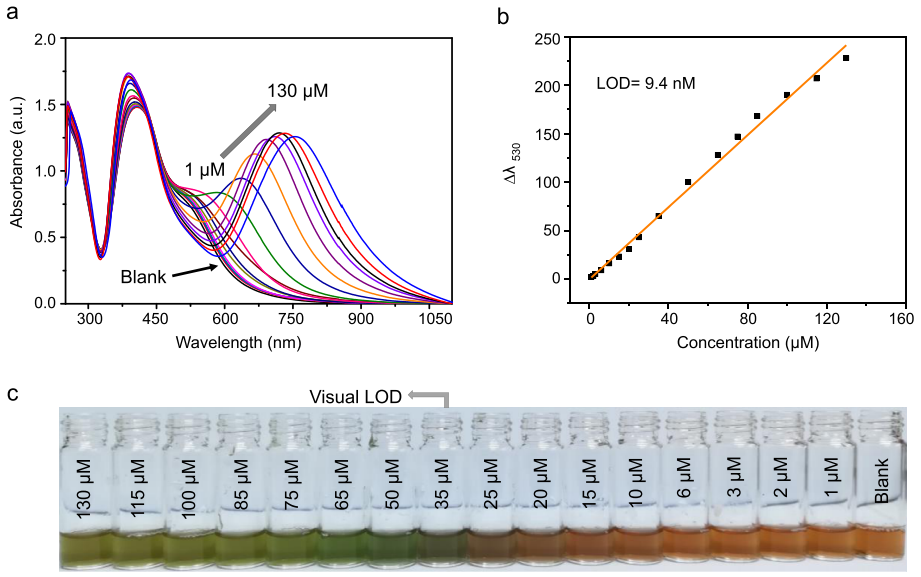

Figure 2. (a) UV−vis spectra of the dual AgNP sensor probe for varying amounts of citrate anions in distilled water, (b) the corresponding standard calibration, and (c) photos demonstrating the visual detection of citrate.

polyethylene oxide. This dual-surfactant system enables highly sensitive and selective colorimetric detection of citrate. For comparison with previous reports, the limit of detection (LOD) of citrate was 4.05 nM in deionized (DI) water, which is, to the best of our knowledge, the lowest LOD in the literature. The limit of visual detection by means of the naked-eye observation was 25 μM. Furthermore, the detection of citrate in urine samples was tested for practical applications, showing an LOD of 14.4 nM. The proposed sensing scheme was applied to develop a paper-based sensor for development of an inexpensive and convenient point-of-care detection tool.

2. RESULTS AND DISCUSSION

2.1. Characterization of the GFEO Surfactant and the Dual-AgNP Sensor. The chemical structure of the synthesized GFEO surfactant was confirmed by Fourier transform infrared (FTIR) and ^{1}H NMR spectroscopy. The FTIR spectra confirm the formation of the new ester carbonyl in addition to loss of both carboxylic carbonyl and carboxylic hydroxyl groups, while ^{1}H NMR verifies the proton distribution of the prepared GFEO-surfactant and the presence of the aliphatic hydrophobic tail (Figure S1a,b, Supporting Information).

The AgNPs were synthesized via photo-reduction using sunlight as a reducing agent. The synthesis mechanism is briefly described in a previous work,[24] where sunlight induces the radiolysis of water to hydrogen, hydrogen peroxide,

https://dx.doi.org/10.1021/acsomega.9b04199
ACS Omega 2020, 5, 10696−10703

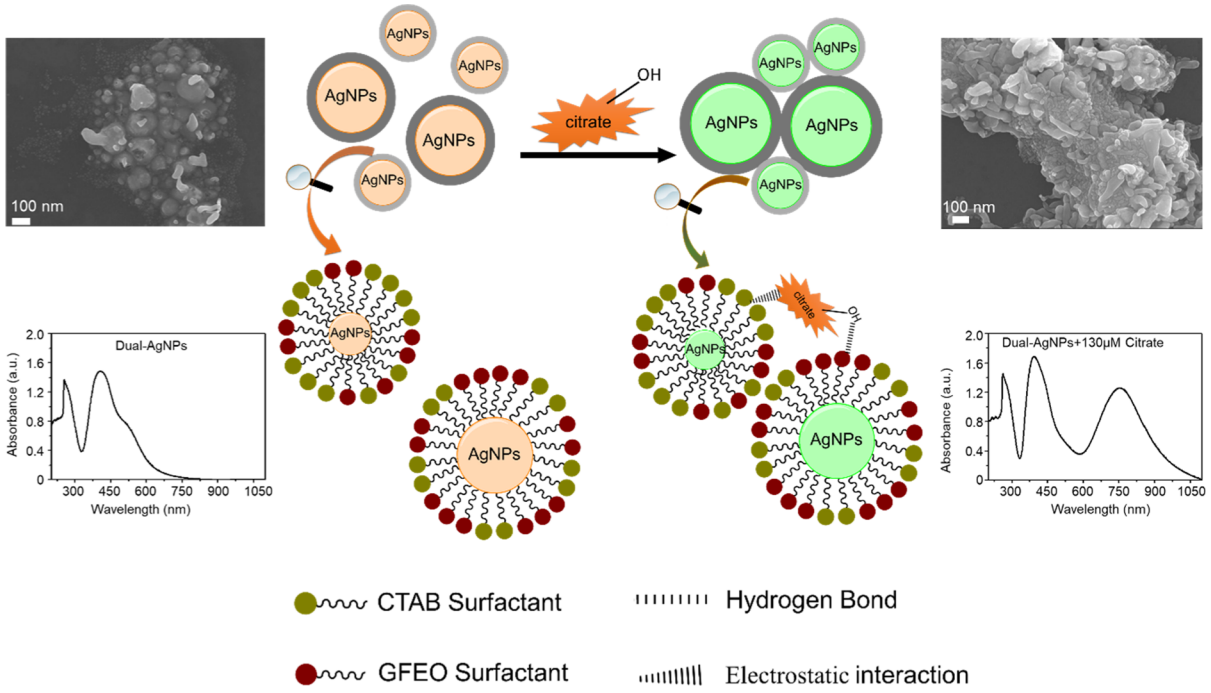

Figure 3. Schematic representation of the citrate-induced AgNP aggregation of the prepared dual AgNP sensor.

hydrogen radicals, hydroxyl radicals, and solvated electrons. The concentrations of the produced solvated electrons, $H^{\bullet}$ atoms, and hydrogen peroxide are, however, very low. Therefore, the CTAB and GFEO surfactants are needed to increase the concentrations of solvated electrons and hydrogen peroxide based on Le Chatelier's principle.

When CTAB was used as an individual capping agent, the synthesized AgNPs exhibited a single absorption peak at 360 nm, with an average particle diameter of 90 ± 60 nm (Figure 1a). When the GFEO surfactant was used as an individual capping agent, a single absorption peak at 381 nm was observed (an average particle diameter of 120 ± 80 nm) (Figure 1b). In contrast, when a mixture of CTAB and GFEO surfactants was used as a dual capping agent, the UV−vis spectrum showed two absorption bands at λ = 405 and 530 nm (Figure 1c, bottom image), indicating the formation of polydispersed AgNPs. The SEM image (Figure 1c, upper image) exhibits the presence of two particles of different sizes, where large particles (115 ± 50 nm) are surrounded by a number of small particles (25 ± 20 nm). The dynamic light scattering (DLS) results confirm the polydispersity of the dual-AgNPs with a polydispersity index (PDI) of 0.851, whereas the synthesized CTAB-AgNPs and GFEO-AgNPs have low PDI values of 0.211 and 0.341, respectively. The zeta potential of CTAB-AgNPs, dual-AgNPs, and G-AgNPs is equal to 61.5 ± 9, 48.2 ± 10, and −10.6 ± 5.6 mV, respectively.

The polydispersed AgNPs obtained in the case of the dual surfactants are because of the mixed surfactant behavior in solution. The dual surfactants attracted each other in solution by van der Waals interactions between hydrophobic tails of CTAB and GFEO and by ion−dipole interactions between hydrophilic heads of CTAB and hydrophilic heads of nonionic GFEO.[25−27] These interactions cause small AgNPs to cluster around large AgNPs. Small AgNPs are formed because of the decrease of interfacial tension of the dual-surfactant colloid system and a high adsorption affinity to the surface of newly formed AgNP nuclei compared to mono CTAB or GFEO surfactants,[28] thus facilitating higher adsorption of mixed surfactants on the AgNP nuclei, hindering their further growth. This difference in the size of AgNPs depending on the surfactants used for synthesis plays an important role in selectivity toward citrate.

2.2. Sensitivity of the Dual-AgNP Sensor. Quantitative analyses of sensitivity of the developed dual-AgNP sensor were conducted by spiking different amounts of citrate anion solution into the dual-AgNP sensor and monitoring by UV−vis spectroscopy (Figure 2a). When the citrate concentration increases, there are changes in both the intensity of the peak at 405 nm and the red shift of the peak at 530 nm. For quantitative detection of citrate, the peak shift at 530 nm was used. The plot of $\Delta\lambda_{530}$ as a function of citrate concentration shows an LOD of 9.4 nM with a linear correlation coefficient (R^2) of 0.99 over a dynamic concentration range of 1−130 μM (Figure 2b) based on the equation $n\sigma/m$, where σ is the standard deviation of the blank sample, m is the slope of the calibration curve, and n is equal to 3. With the incremental injection of the citrate anion, the yellowish color of the dual-AgNP sensor gradually changed to green. Based on the naked eye observation, the limit of visual detection was 35 μM, as shown in Figure 2c.

The colorimetric detection is based on the aggregation of AgNPs upon addition of citrate. Distinct, well-distributed small and large AgNPs (Figure 3a, left image) become fused after injection of 130 μM of citrate (Figure 3a, right image), indicating induced aggregation of AgNPs by citrate. The hydroxyl group in the citrate ion forms a strong hydrogen bond with the ethylene oxide in the GFEO surfactant, and the negative carboxylate center in the citrate anion electrostatically interacts with the positive ammonium group of the CTAB surfactant, both of which induce AgNP aggregation. This observation was confirmed using the transmission electron microscopy (TEM) image (Figure S2, Supporting Information) and DLS measurement (Figure S3, Supporting Information).

https://dx.doi.org/10.1021/acsomega.9b04199
ACS Omega 2020, 5, 10696−10703

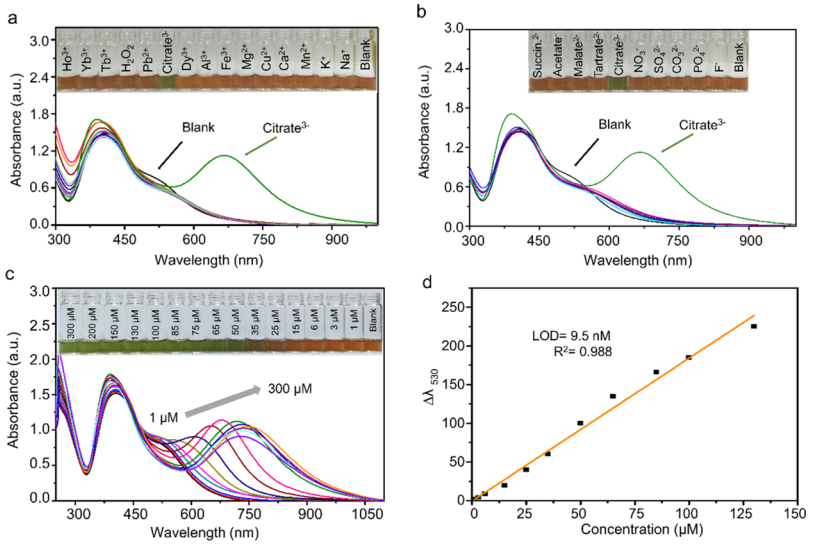

Figure 4. UV−vis response of the dual-AgNP sensor with (a) various metal cations (the inset figure refers to color selectivity) and (b) various anions (the inset figure refers to color selectivity). (c) UV−vis response of the dual-AgNP sensor with different concentrations of citrate in tap water (the inset figure refers to the color change with citrate in the copresence of different cations and anions present in tap water) and (d) the corresponding linear calibration curve between $\Delta\lambda_{530}$ and the citrate concentration (n = 3) in tap water.

Table 1. Comparison of the Citrate Sensors in Terms of Sensing Performance

substrate	method	linear range (μM)	LOD (nM)	refs.
Fe^{3+}MAPcCl-P-n-BA/EIS	electrochemical	1−100,000	400	29
ZnMAPc-G/graphite electrode	electrochemical	0.8−10000	500	30
DPP-Py1 (organic receptor)	fluorescent	0−40	180	31
DTPA-TPY-Zn (organic receptor)	fluorescent	0−10	350	32
TPE-Py (organic receptor)	fluorescent	0−5	100	33
organic rhodamine & Pb_2^+ complex	fluorescent	0.1−50	25	14
organic Rh_B & Mo^{6+} complex	Colorimetric	0.17−12.2	20	34
Rh_B-PMA (organic receptor)	fluorescent and colorimetric	0.053−0.83	6	35
NEDA-Ag-NPs	fluorescent	12−44	26,700	17
dual-AgNPs		1−130	9.4	this work
dual-AgNPs-2×	colorimetric	1−130	6.26	this work
dual-AgNPs-4×		1−85	4.05	this work

2.3. Selectivity and Interference Study of the Dual-AgNP Sensor. To investigate the selectivity of the prepared dual-AgNP sensor toward citrate detection, several interfering cations and anions were tested under the conditions described in Section 4.4. Neither the monosurfactant capped AgNPs (i.e., CTAB-AgNPs and GFEO-AgNPs) nor a mixture of CTAB-AgNPs and GFEO-AgNPs showed specificity toward citrate, as shown in Figure S4 (Supporting Information). Unlike the monosurfactant capped AgNPs, the dual-AgNP sensor exhibited a color change selectively in the presence of citrate ions and did not respond to the other interfering compounds (Figure 4a,b).

Furthermore, to study the interference effect of the copresence of cations and anions against citrate detection on the developed dual-AgNP sensor, tap water containing a number of cations and anions was used. The response of the fabricated dual-AgNP sensor toward citrate in tap water was characterized using UV−vis spectroscopy (Figure 4c), with a linear calibration curve of the correlation coefficient (R^2) 0.989 (Figure 4d), indicating a negligible effect of the interference with the dual-AgNP sensor on citrate detection. The dual-AgNP sensor has comparable sensitivity in distilled water and tap water, with LODs of 9.4 and 9.5 nM, respectively, reflecting the high selectivity of the developed dual-AgNP sensor toward the citrate assay even in the presence of interfering species.

2.4. Optimization of the Dual-AgNP Sensor for Enhancement of Sensing Performance. The prepared dual-AgNP sensor was optimized by diluting the as-synthesized dual-AgNP solution two, four, eight, and ten times (v/v) to obtain dual-AgNPs-2×, dual-AgNPs-4×, dual-AgNPs-8×, and dual-AgNPs-10×, respectively. The concentration of the synthesized dual-AgNPs was calculated and was equal to 20.8 nM. The UV−vis and colorimetric responses based on the dilution of AgNPs are shown in Figure S5 (Supporting Information), with calculated LODs of 6.26, 4.05, 10.27, and 17.61 nM for the dual-AgNPs-2×, dual-AgNPs-4×, dual-AgNPs-8×, and dual-AgNPs-10×, respectively. The dual-AgNPs-4× showed the lowest LOD among all the tested samples. This LOD of 4.05 nM is the lowest value among those of all the previously reported citrate sensors, as depicted in Table 1 and the lowest visual detection limit is 25 M (Figure S5b, Supporting Information).

2.5. Fabrication of the Paper-Based Citrate Sensor. For broader applicability, the dual-AgNP sensor was immobilized on a filter paper to fabricate a paper-based citrate

https://dx.doi.org/10.1021/acsomega.9b04199
ACS Omega 2020, 5, 10696−10703

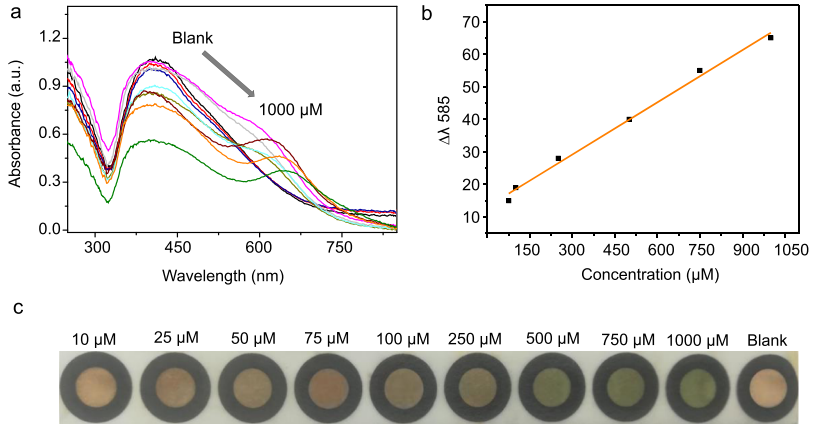

Figure 5. (a) UV−vis spectra of the paper-based dual-AgNP sensor with different concentrations of citrate (10−1000 μM), (b) linear calibration between $\Delta\lambda_{585}$ and the citrate concentration, and (c) photo demonstrating the visual detection of citrate using paper-based dual-AgNPs.

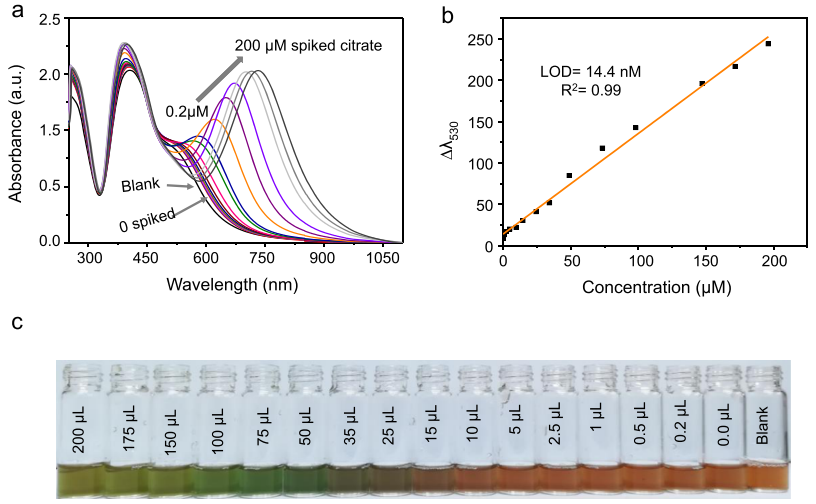

Figure 6. (a) UV−vis spectra of the dual-AgNP sensor with different amounts of spiked citrate in urine (concentration of the zero-spiked sample: 11.4 μM), (b) the linear standard calibration change at $\Delta\lambda_{530}$ of the dual-AgNP sensor, and (c) photo of the visual detection of citrate in urine.

sensor. The undiluted dual-AgNPs were used because they show the most vivid colorimetric change upon target binding. The fabricated paper-based dual-AgNP sensor (Figure S6, Supporting Information) was used for the detection of citrate in DI water at various concentrations from 10 to 1000 μM. Figure 5a outlines the UV−vis response of the fabricated paper-based dual-AgNP sensor upon addition of 20 μL of the citrate-containing solutions with concentrations from 10 to 1000 μM, showing R^2 of 0.99 and a LOD of 10.1 μM (Figure 5b). The paper citrate sensor showed a naked-eye visual detection limit of 250 μM (Figure 5c).

2.6. Citrate Detection in the Urine Samples. To investigate the applicability of the proposed dual-AgNP sensor, we tested citrate detection in urine (100 times diluted). Different volumes of 1 mM citrate were spiked into the dual-AgNP sensor, and the absorbance change was monitored by UV−vis measurement (Figure 6a). The linear change in wavelength at λ = 530 nm as a function of added citrate (Figure 6b) was used to quantify the concentration of citrate in urine. To show the validity of the sensor, a recovery test was performed where three concentrations of the citrate anion (5, 25, and 40 μM) were spiked into the urine sample, and the concentration was determined using the standard addition method. As depicted in Table 2, the results show a recovery mean of 99.6%, indicating high applicability and sensitivity of the proposed sensor for urine samples. Figure 6c shows the change in the color of the prepared dual-AgNP sensor with increasing amounts of spiked citrate in the urine sample.

Table 2. Analytical Results of Citrate Detection in Urine Using the Dual-AgNP Sensor

sample	sensor	detected (μM)	added (μM)	found (μM)	recovery (%)
urine	dual-AgNPs	11.48	5	16.51	100.7
			25	35.91	98.65
			40	51.12	99.45

3. CONCLUSION

In conclusion, a simple, highly selective, and sensitive colorimetric sensor for citrate detection was developed based on the dual-surfactant-capped AgNPs. The combined dual surfactants on AgNPs exhibit high selectivity toward citrate detection, likely arising from hydrogen bond interactions of GFEO and electrostatic binding of CTAB toward citrate. After optimization, the developed dual-surfactant sensor exhibits a visual detection limit of 25 μM by the naked eye readout and a LOD of 4.05 nM by UV−vis measurements, which are the best

https://dx.doi.org/10.1021/acsomega.9b04199
ACS Omega 2020, 5, 10696−10703

Scheme 1. Reaction Pathway of the Gemini Nonionic Surfactant (GFEO)

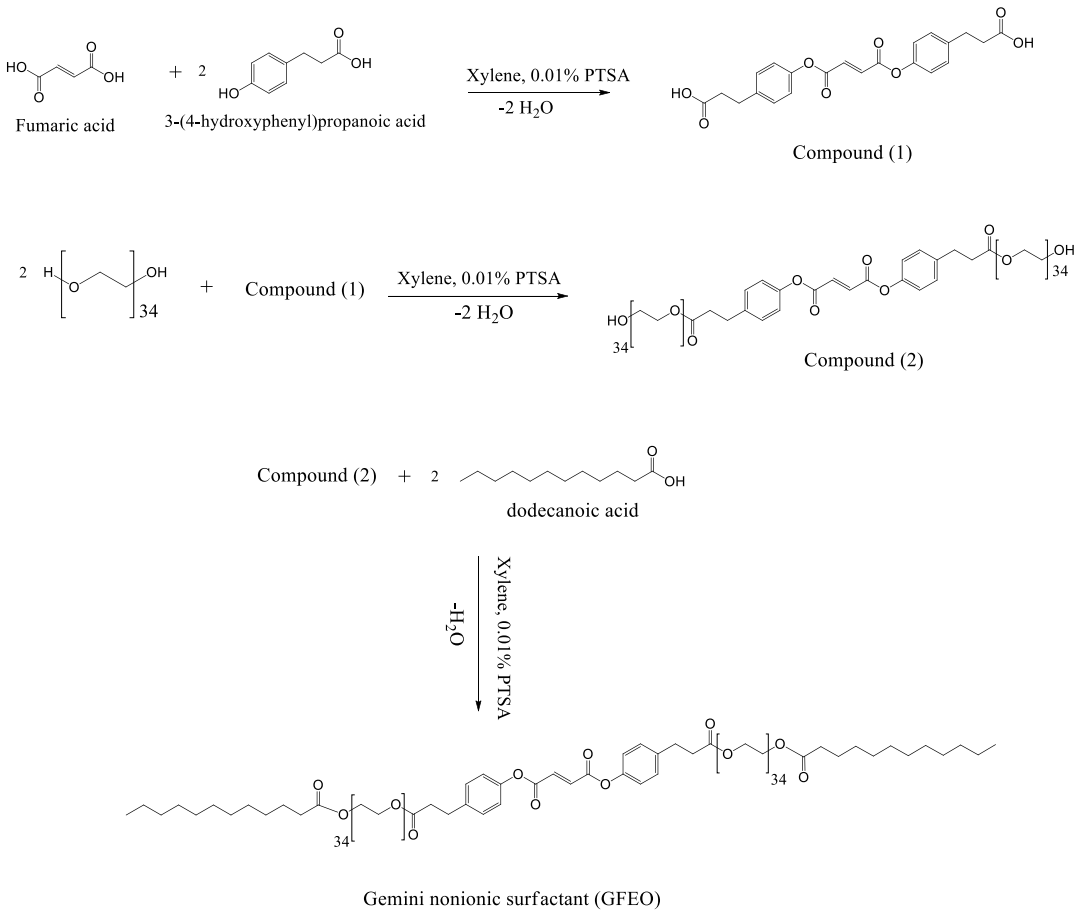

detection sensitivity of citrate in the literature. There was little difference between the LOD of the citrate assay using the developed dual-AgNP sensor in distilled water and in tap water, reflecting its extraordinarily high selectivity toward citrate. Additionally, the dual-AgNP sensor showed a high recovery value in urine, demonstrating its real-life applicability. Finally, a solid-phase dual-AgNP sensor was constructed on a filter paper, showing a satisfactory LOD of 10.1 μM using a UV−vis spectrometer and a low naked-eye LOD of 250 μM. Thus, the developed dual-AgNP sensor can be used as an affordable and portable on-site kit for citrate detection without complicated protocols.

4. MATERIALS AND METHODS

4.1. Materials. Silver nitrate ($AgNO_3$), calcium chloride dihydrate ($CaCl_2{\cdot}2H_2O$), sodium nitrate ($NaNO_3$), potassium chloride (KCl), manganese chloride ($MnCl_2$), copper II chloride dihydrate ($CuCl_2{\cdot}2H_2O$), magnesium chloride anhydrous ($MgCl_2$), aluminum chloride ($AlCl_3$), iron III chloride ($FeCl_3$), dysprosium III chloride hexahydrate ($DyCl_3{\cdot}6H_2O$), sodium citrate tribasic tetrahydrate ($HOC(COONa)(CH_2COONa)_2{\cdot}4H_2O$), hydrogen peroxide ($H_2O_2$), terbium III chloride hexahydrate ($TbCl_3{\cdot}6H_2O$), ytterbium III chloride hexahydrate ($YbCl_3{\cdot}6H_2O$), holmium III chloride hexahydrate ($HoCl_3\ {\cdot}6H_2O$), lead chloride ($PbCl_2$), sodium carbonate anhydrous (Na_2CO_3), sodium phosphate (Na_3PO_4), sodium sulfate (Na_2SO_4), sodium fluoride (NaF), sodium acetate (CH_3COONa), disodium tartrate, disodium succinate, disodium malate, CTAB, polyethylene glycol 1500, and dodecanoic acid were purchased from Sigma-Aldrich Company (South Korea). Fumaric acid, *p*-toluene sulfonic acid (PTSA), and 3-(4-hydroxyphenyl)propanoic acid were purchased from Merck (Germany). All solvents and chemicals were used as received without purification. DI water filtered to 18 MΩ·cm was used in all experiments.

4.2. Preparation of the Polyethylene Oxide Multicarbonyl Gemini Nonionic Surfactant. Fumaric acid (0.01 M, 1.16 g) was esterified with 3-(4-hydroxyphenyl) propanoic acid (0.02 M, 3.32 g) in the presence of 0.01 g PTSA as a catalyst and 100 mL xylene as a solvent using a Dean−Stark apparatus. The reaction was completed when the theoretical amount of water (0.36 mL) was collected in the Dean−Stark apparatus to obtain the diester compound **1** (Scheme 1) after evaporating the solvent and recrystallizing using diethyl ether. Compound **1** (0.003 M, 1.23 g) was esterified with polyethylene glycol 1500 (0.006 M, 9 g) using the same conditions as in the previous step. The reaction was completed when 0.22 mL water was collected in the Dean−Stark apparatus. The obtained product (compound **2**, Scheme 1) was treated as described for compound **1**.[36] Compound **2** (0.003 M, 10 g) was dissolved in 100 mL xylene, with dodecanoic acid (0.006 M, 1.2 g) and 0.01 g PTSA as catalysts. The reaction was completed when 0.22 mL water was collected in the Dean−Stark apparatus. Diethyl ether was used for recrystallization after solvent evaporation and purification. The obtained compound was labeled the GFEO surfactant, as described in Scheme 1.

https://dx.doi.org/10.1021/acsomega.9b04199
ACS Omega 2020, 5, 10696−10703

4.3. Preparation of the Colorimetric Dual-AgNP Sensors. AgNPs were prepared according to a previously reported work with some modifications.[18] In brief, 50 mL of the CTAB aqueous solution (0.4 mM) was mixed with 50 mL of the GFEO surfactant solution (0.2 mM), and the mixture was stirred for 5 min. To the aforementioned solution, 100 mL of the $AgNO_3$ aqueous solution (2 mM) was added and stirred for another 5 min, and then the solution was exposed to sunlight, a green reducing agent. Within five minutes, a rapid color change from colorless to yellowish color occurred, indicating the formation of AgNPs (referred to as the dual-AgNP sensor).

AgNP colloids capped with mono the CTAB or GFEO surfactant were prepared separately using the same procedure described in the preparation of the dual-AgNPs sensor and are referred to as CTAB-AgNPs and GFEO-AgNPs, respectively.

4.4. Characterization of the Surfactant and AgNPs. The chemical structure of the synthesized GFEO surfactant was tested by Bruker FTIR (model IFS-66/S, TENSOR27) and Bruker FT-NMR spectroscopy (model AVANCE III 700). The morphology of the prepared AgNPs was examined using a TEM (model JEM ARM 200 F JEOL) and a scanning electron microscope (model JSM7500F) at an accelerating voltage of 15 kV. The Zetasizer Ver. 7.11 (Malvern Zetasizer Nano Instruments Ltd, Worcestershire, UK) was used to examine the size distribution of the synthesized NPs based on DLS. Absorbance of the prepared NPs was monitored by UV−vis spectroscopy (JASCO V 770, Japan).

4.5. Sensitivity and Selectivity of the Citrate Sensors. A stock solution was prepared from the citrate anion aqueous solution (1 mM) and was used to prepare citrate of final concentrations ranging from 1 to 130 μM. Different quantities of 1 mM citrate solution (1, 3, 6, 15, 25, 35, 50, 65, 85, 100, 115, and 130 μL) were injected into the citrate sensor to yield a final volume of 1 mL. Changes in the absorption spectra of AgNPs were monitored with UV−vis spectroscopy in the range from 200 to 1100 nm in addition to monitoring the color change visually by the naked eye.

To examine the specificity of the prepared dual-AgNP sensor, various inorganic cations, inorganic anions, and organic anions were tested individually under the same experimental conditions. For this, 200 μM solutions of the different ions (Na^+, K^+, Mn^{2+}, Ca^{2+}, Cu^{2+}, Mg^{2+}, Al^{3+}, Fe^{3+}, Gd^{3+}, Nd^{3+}, Dy^{3+}, Li^+, Pb^{2+}, H_2O_2, Tb^{3+}, Yb^{3+}, Ho^{3+}, CO_3^{2-}, PO_4^{2-}, SO_4^{2-}, F^-, CH_3COO^-, succinate^{2-}, malate^{2-}, and tartrate^{2-}) were used. The absorbance and color changes were measured 30 min after adding the analytes to the prepared dual-AgNP sensor.

An interference test using tap water was conducted because tap water contains various cations and anions. A stock solution of citrate (1 mM) in tap water was prepared, after which varying amounts of citrate anions (final concentrations of 1−300 μM) were spiked in the dual-AgNP sensor under the same experimental conditions.

4.6. Fabrication of a Paper-Based Sensor Using the Dual-AgNP Sensor. Whatman filter paper (20 cm × 20 cm) was used for the construction of a paper-based analytical device as a solid sensor for the visual detection of citrate using the prepared dual-AgNP sensor. First, a hydrophilic zone was created on a paper sheet by printing a hydrophobic circular region with waxy ink using a laser printer. After printing, the paper sheet was cut and immersed in water for 5 min. Next, 100 μL (3 times for 5 min each) of the as-prepared dual-AgNP sensor was placed on the wet hydrophilic zone and dried in air to obtain the paper-based analytical device of dual-AgNPs (referred to as the paper-based dual-AgNP sensor).

4.7. Detection of Citrate in Urine. To investigate the applicability of the proposed sensors for citrate detection, a human urine sample was used as a real example of a biological matrix. The human urine sample was obtained from a volunteer and centrifuged at 4000 rpm for 20 min before the detection of the citrate anion using the standard addition method, where known volumes of the known citrate concentrations (1 mM) were spiked in the diluted urine sample (100 times) to test the ability to determine the concentration of unknown citrate in the urine sample. The recovery rate (%) was calculated to determine the feasibility of the dual-AgNP sensor using the following equation

$$\text{Recovery rate (\%)} = \frac{\text{measured concentration}}{\text{spiked concentration}} \times 100$$

■ ASSOCIATED CONTENT

Supporting Information

The Supporting Information is available free of charge at https://pubs.acs.org/doi/10.1021/acsomega.9b04199.

FTIR and ^{1}H NMR spectra of the prepared GFEO surfactant, TEM and DLS of the prepared dual-AgNP sensor with and without citrate, and dual-AgNP sensor optimization (PDF)

■ AUTHOR INFORMATION

Corresponding Authors

Jun Young Lee − *School of Chemical Engineering, Sungkyunkwan University, Suwon 16419, Republic of Korea*; Email: jylee7@skku.edu

Dong-Hwan Kim − *School of Chemical Engineering and Biomedical Institute for Convergence at SKKU (BICS), Sungkyunkwan University, Suwon 16419, Republic of Korea*; orcid.org/0000-0002-2753-0955; Email: dhkim1@skku.edu

Author

Samy M. Shaban − *School of Chemical Engineering and Biomedical Institute for Convergence at SKKU (BICS), Sungkyunkwan University, Suwon 16419, Republic of Korea*

Complete contact information is available at: https://pubs.acs.org/10.1021/acsomega.9b04199

Notes

The authors declare no competing financial interest.

■ ACKNOWLEDGMENTS

This work was financially supported by a National Research Foundation of Korea (NRF) grant funded by the Ministry of Education, Science, and Technology (NRF-2018R1D1A1B07041584).

■ REFERENCES

(1) Türkoğlu, Ş. Genotoxicity of five food preservatives tested on root tips of Allium cepa L. *Mutat. Res., Genet. Toxicol. Environ. Mutagen.* **2007**, *626*, 4−14.

(2) Araújo, C. L.; Melo, E. I.; Coelho, N. M. M. Potentiometric detection of citrate in beverages using a graphite carbon electrode. *Talanta* **2011**, *84*, 1169−1173.

(3) Liu, Z.-H.; Devaraj, S.; Yang, C.-R.; Yen, Y.-P. A new selective chromogenic and fluorogenic sensor for citrate ion. *Sens. Actuators, B* **2012**, *174*, 555−562.
(4) Cebotaru, V.; Kaul, S.; Devuyst, O.; Cai, H. U. I.; Racusen, L.; B Guggino, W.; E Guggino, S. High citrate diet delays progression of renal insufficiency in the ClC-5 knockout mouse model of Dent's disease. *Kidney Int.* **2005**, *68*, 642−652.
(5) Schell-Feith, E. A.; Moerdijk, A.; van Zwieten, P. H. T.; Zonderland, H. M.; Holscher, H. C.; Kist-van Holthe, J.; van der Heijden, B. J. Does citrate prevent nephrocalcinosis in preterm neonates? *Pediatr. Nephrol.* **2006**, *21*, 1830−1836.
(6) Costello, L. C.; Franklin, R. B. Prostatic fluid electrolyte composition for the screening of prostate cancer: a potential solution to a major problem. *Prostate Cancer Prostatic Dis.* **2008**, *12*, 17.
(7) Gupta, A.; Mahdi, A. A.; Ahmad, M. K.; Shukla, K. K.; Jaiswer, S. P.; Shankhwar, S. N. 1H NMR spectroscopic studies on human seminal plasma: A probative discriminant function analysis classification model. *J. Pharmaceut. Biomed.* **2011**, *54*, 106−113.
(8) Dittrich, R.; Kurth, J.; Decelle, E. A.; DeFeo, E. M.; Taupitz, M.; Wu, S.; Wu, C.-l.; McDougal, W. S.; Cheng, L. L. Assessing prostate cancer growth with citrate measured by intact tissue proton magnetic resonance spectroscopy. *Prostate Cancer Prostatic Dis.* **2012**, *15*, 278.
(9) Kelebek, H.; Selli, S.; Canbas, A.; Cabaroglu, T. HPLC determination of organic acids, sugars, phenolic compositions and antioxidant capacity of orange juice and orange wine made from a Turkish cv. Kozan. *Microchem. J.* **2009**, *91*, 187−192.
(10) do Nascimento, R. F.; Selva, T. M. G.; Ribeiro, W. F.; Belian, M. F.; Angnes, L.; do Nascimento, V. B. Flow-injection electrochemical determination of citric acid using a cobalt(II)-phthalocyanine modified carbon paste electrode. *Talanta* **2013**, *105*, 354−359.
(11) Awasthi, S.; Srivastava, A.; Singla, M. L. Voltammetric determination of citric acid and quinine hydrochloride using polypyrrole-pentacyanonitrosylferrate/platinum electrode. *Synth. Met.* **2011**, *161*, 1707−1712.
(12) Ghosh, K.; Sen, T.; Fröhlich, R. A naphthyridine-based receptor for sensing citric acid. *Tetrahedron Lett.* **2007**, *48*, 2935−2938.
(13) Amendola, V.; Bergamaschi, G.; Buttafava, A.; Fabbrizzi, L.; Monzani, E. Recognition and Sensing of Nucleoside Monophosphates by a Dicopper(II) Cryptate. *J. Am. Chem. Soc.* **2010**, *132*, 147−156.
(14) Li, C.-Y.; Zhou, Y.; Li, Y.-F.; Kong, X.-F.; Zou, C.-X.; Weng, C. Colorimetric and fluorescent chemosensor for citrate based on a rhodamine and Pb2+ complex in aqueous solution. *Anal. Chim. Acta* **2013**, *774*, 79−84.
(15) Zhu, Z.; Zhou, J.; Li, Z.; Yang, C. Dinuclear zinc complex for fluorescent indicator-displacement assay of citrate. *Sens. Actuators, B* **2015**, *208*, 151−158.
(16) Sun, Y. K.; Yao, X. L.; Zhong, C.; Xue, P.; Fu, E. Colorimetric sensing ensemble for citrate in water. *Sens. Actuators, B* **2014**, *194*, 269−275.
(17) Choudhury, R.; Purkayastha, A.; Debnath, D.; Misra, T. K. Synthesis and study of aggregation kinetics of fluorescence active N-(1-Naphthyl)ethylenediammonium cations functionalized silver nanoparticles for a chemo-sensor probe. *J. Mol. Liq.* **2017**, *238*, 96−105.
(18) Shaban, S. M.; Aiad, I.; El-Sukkary, M. M.; Soliman, E. A.; El-Awady, M. Y. One step green synthesis of hexagonal silver nanoparticles and their biological activity. *J. Ind. Eng. Chem.* **2014**, *20*, 4473−4481.
(19) Wettig, S. D.; Verrall, R. E. Thermodynamic Studies of Aqueous m−s−m Gemini Surfactant Systems. *J. Colloid Interface Sci.* **2001**, *235*, 310−316.
(20) Qiu, L.-G.; Xie, A.-J.; Shen, Y.-H. A novel triazole-based cationic gemini surfactant: synthesis and effect on corrosion inhibition of carbon steel in hydrochloric acid. *Mater. Chem. Phys.* **2005**, *91*, 269−273.
(21) Aiad, I.; Shaban, S. M.; Moustafa, H. Y.; Hamed, A. Experimental Investigation of Newly Synthesized Gemini Cationic Surfactants as Corrosion Inhibitors of Mild Steel in 1.0 M HCl. *Prot. Met. Phys. Chem. Surf.* **2018**, *54*, 135−147.
(22) Xu, J.; Hu, J.; Peng, C.; Liu, H.; Hu, Y. A simple approach to the synthesis of silver nanowires by hydrothermal process in the presence of gemini surfactant. *J. Colloid Interface Sci.* **2006**, *298*, 689−693.
(23) Liu, Q.; Guo, M.; Nie, Z.; Yuan, J.; Tan, J.; Yao, S. Spacer-Mediated Synthesis of Size-Controlled Gold Nanoparticles Using Geminis as Ligands. *Langmuir* **2008**, *24*, 1595−1599.
(24) Aiad, I.; El-Sukkary, M. M.; Soliman, E. A.; El-Awady, M. Y.; Shaban, S. M. In situ and green synthesis of silver nanoparticles and their biological activity. *J. Ind. Eng. Chem.* **2014**, *20*, 3430−3439.
(25) Negm, N. A.; Sabagh, A. M. E. Interaction between cationic and conventional nonionic surfactants in the mixed micelle and monolayer formed in aqueous medium. *Quím. Nova* **2011**, *34*, 1007−1013.
(26) Holland, P. M.; Rubingh, D. N. Mixed Surfactant Systems. *Mixed Surfactant Systems*; American Chemical Society, 1992; Vol. *501*, pp 2−30.
(27) Lee, B. H. Effects of Various Alcohols and Salts on the Mixed Micellization of Cationic Surfactant (CPC) with Nonionic Surfactant (TX-100). *Colloid Interface Sci. Commun.* **2017**, *19*, 1−4.
(28) Li, J.; Li, Y.; Song, Y.; Wang, Z.; Zhang, Q. Properties of quaternary ammonium surfactant with hydroxyethyl group and anionic surfactant mixed systems. *J. Mol. Liq.* **2018**, *271*, 373−379.
(29) Azzouzi, S.; Ben Ali, M.; Abbas, M. N.; Bausells, J.; Zine, N.; Errachid, A. Novel iron (III) phthalocyanine derivative functionalized semiconductor based transducers for the detection of citrate. *Org. Electron.* **2016**, *34*, 200−207.
(30) Nooredeen, N. M.; Abd El-Ghaffar, M. A.; Darwish, W. M.; Elshereafy, E.; Radwan, A. A.; Abbas, M. N. Graphene oxide with covalently attached zinc monoamino-phthalocyanine coated graphite electrode as a potentiometric platform for citrate sensing in pharmaceutical preparations. *J. Solid State Electrochem.* **2015**, *19*, 2141−2154.
(31) Hang, Y.; Wang, J.; Jiang, T.; Lu, N.; Hua, J. Diketopyrrolopyrrole-Based Ratiometric/Turn-on Fluorescent Chemosensors for Citrate Detection in the Near-Infrared Region by an Aggregation-Induced Emission Mechanism. *Anal. Chem.* **2016**, *88*, 1696−1703.
(32) Jiang, T.; Lu, N.; Hang, Y.; Yang, J.; Mei, J.; Wang, J.; Hua, J.; Tian, H. Dimethoxy triarylamine-derived terpyridine−zinc complex: a fluorescence light-up sensor for citrate detection based on aggregation-induced emission. *J. Mater. Chem. C* **2016**, *4*, 10040−10046.
(33) Liu, C.; Hang, Y.; Jiang, T.; Yang, J.; Zhang, X.; Hua, J. A light-up fluorescent probe for citrate detection based on bispyridinum amides with aggregation-induced emission feature. *Talanta* **2018**, *178*, 847−853.
(34) Tavallali, H.; Deilamy-Rad, G.; Parhami, A.; Hasanli, N. An efficient and ultrasensitive rhodamine B-based reversible colorimetric chemosensor for naked-eye recognition of molybdenum and citrate ions in aqueous solution: Sensing behavior and logic operation. *Spectrochim. Acta, Part A* **2015**, *139*, 253−261.
(35) Tavallali, H.; Baezzat, M.-R.; Deilamy-Rad, G.; Parhami, A.; Hasanli, N. An ultrasensitive and highly selective fluorescent and colorimetric chemosensor for citrate ions based on rhodamine B and its application as the first molecular security keypad lock based on phosphomolybdic acid and citrate inputs. *J. Lumin.* **2015**, *160*, 328−336.
(36) Shaban, S. M.; Aiad, I.; Moustafa, A. H.; Aljoboury, O. H. Some alginates polymeric cationic surfactants; surface study and their evaluation as biocide and corrosion inhibitors. *J. Mol. Liq.* **2019**, *273*, 164−176.

https://dx.doi.org/10.1021/acsomega.9b04199
ACS Omega 2020, 5, 10696−10703